Supporting Information

In situ Photoelectric Biosensing based on Ultra-Narrow-Band Near Infrared Plasmonic Hot Electron Photodetection

Xianghong Nan[1,#], Wenduo Lai[1,#], Jie Peng[2], Haiquan Wang[1], Bojun Chen[1], Huifan He[1], Zekang Mo[1], Zikun Xia[1], Ning Tan[1], Zhong Liu[3], Long Wen[1,*], Dan Gao[2], Qin Chen[1,*]

[1]Guangdong Provincial Key Laboratory of Nanophotonic Manipulation, Institute of Nanophotonics, Jinan University, Guangzhou 511443, China

[2]State Key Laboratory of Chemical Oncogenomics, Shenzhen International Graduate School, Tsinghua University, Shenzhen, Guangdong, 518055, China

[3]College of Life Science and Technology, Jinan University, Guangzhou 510632, China

#equal contribution

*longwen@jnu.edu.cn, chenqin2018@jnu.edu.cn

S1. Narrow-band photodetectors in literatures

The major performance parameters such as operating wavelength (λ_0), full width at half maximum (FWHM), quality (Q) factor of typical narrow-band photodetectors in literatures are summarized in Table S1. It is clear to see that the normalized response bandwidth (FWHM/λ_0) of the plasmonic hot electron (HE) photodetector in this work is much smaller than the reported results. Even the one with several tens of pairs of DBRs [1] has more than twice FWHM/λ_0 of our results. The Q factor of this work is at least one order of magnitude higher than most reported results. Improved sensing and spectral resolution performance can be expected with such a narrow-band plasmonic HE photodetector.

Table S1. Performance parameters of various photodetectors in literatures.

	Mechanism	λ_0(nm)	FWHM (nm)	FWHM/λ_0	Q=λ_0/ FWHM	Ref
Engineering material and device structure	Dye blending	650	80	12.3%	8	[6]
	Charge collection narrowing	570	20	3.5%	29	[7]
	Charge collection narrowing	940	80	8.5%	12	[8]
	Carrier trapping	650	30	4.6%	22	[9]
	Self-trapped state	420	10	2.6%	42	[10]
	Depletion region engineering	1060	107	10%	10	[11]
	Gate transmittance tuning	319	11	3.4%	29	[12]
Integrating photodetector and narrowband filter	DBR resonant cavity	911	4	0.43%	228	[13]
	Metal cavity	5710	95	1.7%	60	[14]
	Metallic nanodisk array	7200	1250	17.4%	6	[15]
	Photonic crystal filter	655	14.8	2.3%	44	[16]
	Metamaterial	2700	300	11.1%	9	[17]
	Nanowires	1560	40	2.6%	39	[18]
	Plasmonic gratings	1470	120	8.2%	12	[21]
	Plasmonic gratings	1230	100	8.1%	12	[22]
	Plasmonic gratings	880	30	3.4%	29	[23]
	Plasmonic gratings	1550	2.6	0.17%	596	This work

S2. Coupled mode theory

The Au/Si gratings can be qualitatively represented by a one-port resonator within the framework of temporal coupled mode theory (CMT). The reflection coefficient can be written as:

$$r = r_0 + \frac{\Gamma_{rad}}{i(\omega-\omega_0)+\Gamma_{total}/2} e^{i\phi} \quad (1)$$

where ω_0 is the resonant frequency, Γ_{rad} is the radiative decay rate, Γ_{abs} is the absorption decay rate, and Γ_{total} is the total decay rate ($\Gamma_{rad} + \Gamma_{abs}$). When incident light is coupled to the gratings, the resonant absorption can be maximized by changing the grating dimensions to match the critical coupling condition, *i.e.*, the absorption loss equals the radiative loss. The results of FDTD simulation can be fitted with the above CMT formula and thus obtain the corresponding decay rates.

S3. Wave vector matching condition

In the proposed plasmonic photodetector structure, surface plasmon resonance (SPR) can be excited by matching the incidence wave vector to that of SPR with the help of Bragg wave vector provided by the Au-Si gratings. The momentum matching condition can be written as:

$$ksin\theta + mG = \pm k_{sp} \tag{2}$$

where θ is the incident angle, G is grating constant ($2\pi/P$), k is the wave vector, m is an integer representing the diffraction order, k_{sp} is the wave vector of SPR. Because the etching depth of the gratings is small, k_{sp} can be approximately calculated using the dispersion relationship of surface plasmon mode supported by the flat Au/dielectric interface:

$$k_{sp} = k\sqrt{\varepsilon_D \varepsilon_{Au}/(\varepsilon_D + \varepsilon_{Au})} \tag{3}$$

where ε_{Au} is the gold relative permittivity and ε_D is the relative permittivity of the surrounding dielectric medium.

According to Eq. (2), for oblique incidence two resonances can be generated, associated with the positive/negative first-order excitation of SPR. With the increase of incidence angle, the positive and negative first-order modes show blue shift and red shift, respectively.

S4. Dynamic responses of plasmonic photodetectors

The plasmonic HE photodetectors show reasonably fast switching as shown in Figure S1.

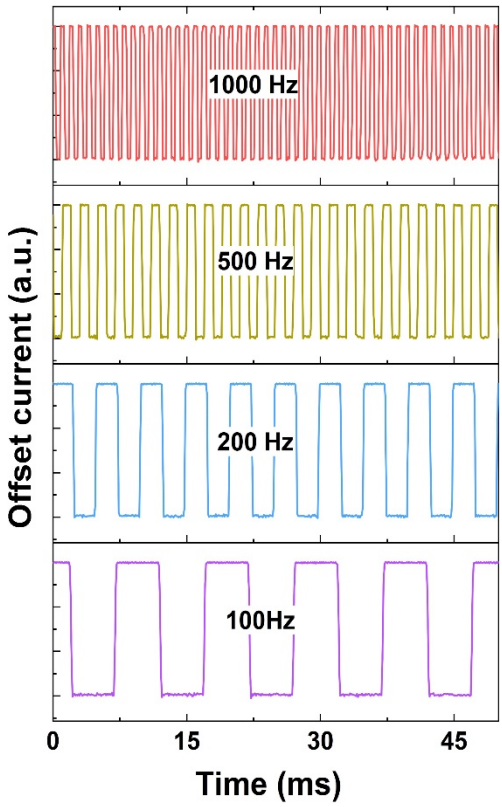

Figure S1. Dynamics responses of the plasmonic photodetectors under fast switching of the laser illumination.

S5. Glucose sensing with different laser sources

Glucose sensing experiments were also conducted on a same device with different laser sources at a wavelength of 1344 nm, where the device linewidth is 6 nm. As shown in Figure S2, the measured offset currents show obvious difference when a NKT supercontinuum laser (FWHM = 12 nm) and a Civil laser (1342 nm, FWHM = 30 pm) were used respectively. As expected, the current signals of a laser with a smaller linewidth are larger than the one with a larger linewidth.

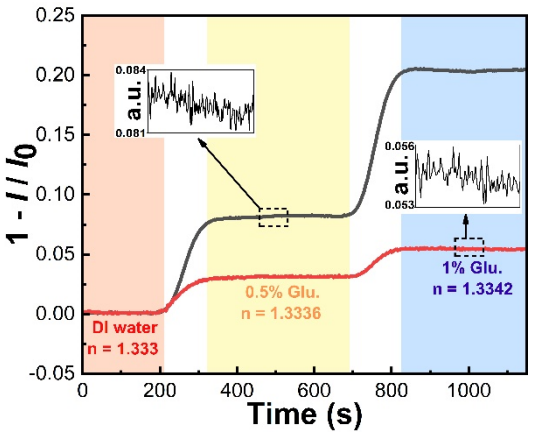

Figure S2. Real-time offset currents measured in glucose sensing experiments with a NKT laser (red line) and a Civil laser (black line) respectively.